Macromolecular Research, Vol. 11, No. 3, pp 163-171 (2003)

Preparation of Composite Membranes of Dense PAA-Poly(BMA-*co*-MMA) IPN Supported on Porous and Crosslinked Poly(BMA-*co*-MMA) Sublayer and Their Pervaporation Characteristics

Sung-Chul Kim*

Center for Advanced Functional Polymers, Korea Advanced Institute of Science and Technology, 373-1, Kusong-dong, Yusong-gu, Daejon 305-701, Korea

Byung-Yun Lim

Research & Development Institute, Honam Petrochemical Corporation, 24-1, Jang-dong, Yusong-gu, Daejon 305-706, Korea

Received Dec. 31, 2002; Revised Apr. 24, 2003

Abstract: For the pervaporation of water-ethanol mixtures, new composite membranes having poly(acrylic acid)-poly(butyl methacrylate-*co*-methyl methacrylate) interpenetrating polymer network [PAA-P(BMA-*co*-MMA) IPN] skin layer supported on porous and crosslinked poly(BMA-*co*-MMA) were prepared. The morphology of the sublayer of the composite membrane prepared in the presence of 60 wt% solvent showed cellular structure, on the other hand that of sublayer prepared in the presence of 70 wt% solvent presented very porous interconnected pore structure with macrovoids. Permeation rates of the composite membranes were largely influenced by the morphology of the sublayer. Separation factors increased with the increase of the degree of crosslinking of the PAA network. It was found that permeation rates could be increased by introducing anionic charges on carboxyl groups of the PAA. The permeation rate changes of the PAA-P(BMA-*co*-MMA) IPN composite membranes according to the feed compositions showed quite similar pattern with the swelling behavior in water-ethanol mixtures.

Keywords: composite membrane, pervaporation, IPN, crosslinked sublayer, separation of water-ethanol mixture.

Introduction

In the concentration of water-ethanol solutions via pervaporation, it is well known that hydrophilic polymer membranes are useful because the selectivity for water could be enhanced, due to the strong interaction between the water molecule and hydrophilic polymers. However, strong interaction between the water molecule and the hydrophilic polymers leads to the swelling of the polymers, and results in the loss of mechanical and selective properties. Crosslinking is a way to prevent excess swelling of the membrane. On the other hand, insufficient swelling due to high degree of crosslinking causes decrease in the permeation rate. Therefore, the ideal material for dehydration of water-ethanol solutions through pervaporation process should have a fine hydrophilic /hydrophobic balance of the affinity and swelling capacity as well as good mechanical properties.[1,2] The concept of the interpenetrating polymer network (IPN) may be applied to combining two polymers with different hydrophilicity.[3]

Some studies were carried out regarding the water-ethanol separation through IPN membranes.

Hydrophilic-hydrophobic PU/PS IPN membranes were synthesized under high pressure and the effect of pressure on the morphology and swelling behavior in water-ethanol mixtures were analyzed.[4] It has also been reported that introducing ionized groups into the membranes could increase the water permselectivity.[5,6] The results for the pervaporation performances of the IPN membranes containing ionic groups [Cationic PU/anionic P(MMA-*co*-AA) IPN] showed that the separation factor increased as the content of anionic component in the membrane increased.[7] The performance of the IPN membranes were studied in comparison to the blend membranes.[8] Models for the simulation of the pervaporation behavior through IPN membranes (SAN/anionic PAA IPN and porous SAN/anionic PAA IPN) were also proposed.[9] However, these works were on symmetric dense IPN membranes resulting in low permeability, especially for a high

*e-mail : kimsc@mail.kaist.ac.kr
1598-5032/06/163-09

ethanol concentration range of the feed composition.[4,7,9,10] It is not necessary to prepare the whole membrane as IPN structure because only the surface layer of the membrane should contribute to the selectivity, and the permeation resistance should be minimized. If we can prepare composite membranes consisting of thin IPN skin layer and porous sublayer, permeation rate could be enhanced. One of the approaches employed is to prepare IPN layer supported on porous sublayer. L. Liang *et al.* investigated the pervaporation of water-ethanol mixtures through the PVA-PAAM IPN composite membranes supported on polyethersulfone.[10] It was found that the supported membranes had higher permeability but a lower selectivity compared to unsupported ones. However, there is no work available in the literature related with IPN composite membrane having IPN skin layer and crosslinked porous sublayer. This is because its hard to obtain crosslinked porous structure.

PAA is well known as a hydrophilic, water-permselective material. However, it can be dissolved or significantly swollen for the low ethanol composition of the feed, resulting in remarkable decrease of permeation rate. Thus, PAA for a membrane material is commonly used as a crosslinked form or an ionic complex structure.[11,12] According to the investigation of Yoshikawa *et al.*,[13] the hydrogen bonding ability towards carboxylic acid decreases in the following order: water > ethanol > acetonitrile. This hydrogen bonding force between water and PAA is stronger than that between ethanol and PAA since the PAA shows preferential water permeation rather than ethanol permeation.

In this study, we prepared series of composite membranes having PAA-P(BMA-*co*-MMA) IPN skin layer supported on crosslinked and porous P(BMA-*co*-MMA) sublayer by a method described in the following section and studied the effect of morphology, degree of crosslinking and anionic charge on pervaporation performances.

Experimental

Materials. Butyl methacrylate (BMA, Aldrich, Milwaukee, WI, USA) for hydrophobic component was used. Methyl methacrylate (MMA, Aldrich, Milwaukee, WI, USA) monomer was used for the purpose of enhancing the T_g of the sublayer. Acrylic acid (AA, Aldrich, Milwaukee, WI, USA) was used for hydrophilic component. The crosslinking agent was ethylene glycol di-methacrylate (EGDMA, Aldrich, Milwaukee, WI, USA). Benzoyl peroxide (BPO, Janssen, Geel, Belgium) was used as a thermal initiator. The solvent *N*-methyl-2-pyrrolidone (NMP, Junsei, Tokyo, Japan) and ethanol (99%, Aldrich, Milwaukee, WI, USA) was used without purification. Water was distilled.

Membrane Preparation and Characterization. The support layer was prepared as the previous paper.[14] For the preparation of IPN composite membrane, following procedure was employed. Mixture containing BMA monomer, MMA monomer, BPO, EGDMA and NMP was polymerized at 80 °C for 24 hrs in a glass mold, which was made up of two glass plates with a PET film spacer. The thickness of the spacer was 100 μm. After polymerization, one of the glass plates of the mold was removed. Then, the mixture containing AA, BPO (1 wt%) and EGDMA was cast onto the surface of the crosslinked poly(BMA-*co*-MMA) sublayer containing NMP solvent. The coated layer was kept in an oven at 80 °C for 30 min for the polymerization of acrylic acid (AA) and crosslinking by EGDMA. After polymerization of the coated layer, it was immediately immersed into water bath at room temperature to exchange solvent with water. After 24 hrs, the layer was dried in air, and finally porous sublayer was obtained. Various composite membranes having different degrees of crosslinking of skin layers and different monomer compositions of the sublayer were prepared. In order to introduce anionic charge into the carboxyl groups of PAA/P(BMA-*co*-MMA) IPN skin layer, membranes were dipped in 5 wt% NaOH aqueous solution at room temperature for 24 hrs. The schematic procedure for preparing composite IPN membrane is presented in Figure 1.

The morphologies of the cross-sections of the membranes were examined by means of SEM (Scanning Electron Microscope, TOPCON SM-701, Tokyo, Japan).

To obtain topographical images of the membranes, a Nanoscope MultiMode AFM (atomic force microscopy) together with an Extender Electronics Module (Digital

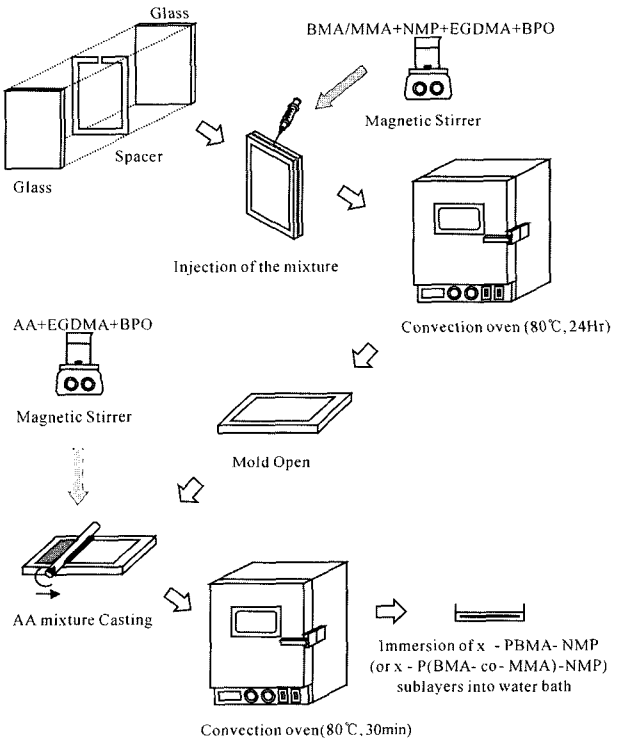

Figure 1. Preparation of PAA/P(BMA-*co*-MMA) IPN composite membranes.

Instrument Co., Santa Barbara, CA, USA) was used. Tapping mode was employed at the cantilever's resonance frequency using a probe cantilever unit composed of silicon (Nanoprobe, cantilever length 125 μm and resonance frequency 291-233 kHz, Santa Barbara, CA, USA).

The compositions of the IPN composite membrane were analyzed by using Fourier Transformation Infrared Spectroscopy (NICOLET, Magma550/NICPLAN, Madison, Michigan, USA) equipped with an optical microscope.

The porosities of the composite membranes were evaluated from the following equation.

$$\text{Porosity} = (V_m - V_p)/V_m \times 100\% = [A \times t - (W_m/\rho_p)]/A \times t\ 100\%$$

where V_m is the volume of the sample, V_p is the volume occupied by polymer and W_m is the mass of the sample. A and t denote the area and thickness of the sample respectively. ρ_p is the density of the polymer (1.113 g/cm^3).

Pervaporation Experiments. The schematic pervaporation apparatus is presented in Figure 2. The feed solution was maintained at 25 °C and the effective membrane area was 19.63 cm^2. The feed solution was circulated from the feed reservoir in a thermostatic bath by the peristaltic pump and stirred in the pervaporation cell by a magnetic stirrer to prevent concentration polarization at the membrane surface. The permeate side was evacuated by a vacuum pump and

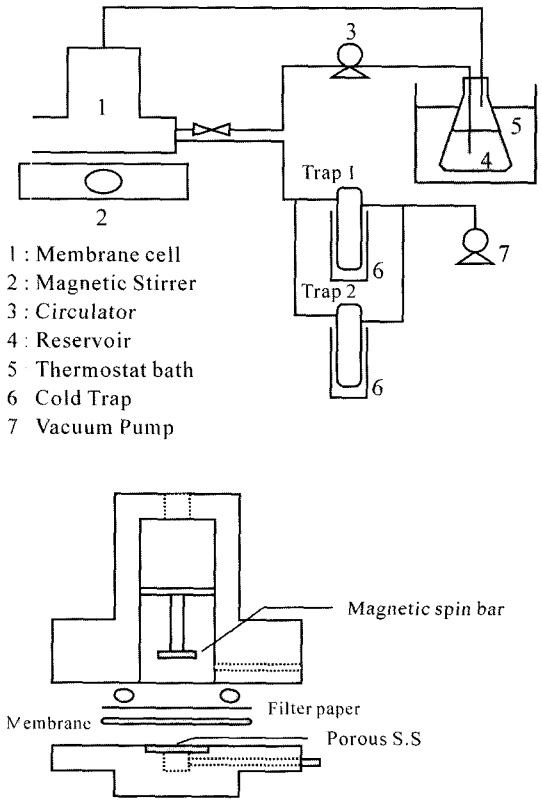

Figure 2. Schematic diagram of the apparatus used for pervaporation experiments.

was maintained below 5 mmHg. In each run, the apparatus was run at least 1 hr without condensation, to reach the steady state before collecting the permeate. The gaseous permeate was collected in a trap chilled with liquid nitrogen, and the permeation rate was calculated from the permeate weight per unit time. The composition analysis of the permeate was done using Karl-Fischer moisture content measurement (Kyoto Electronics, MKC-210, Tokyo, Japan) at 25 °C. A calibration curve of the water-ethanol mixture was prepared using known quantities of the two components. The separation factor (α) of the membrane was calculated using the expression:

$$\alpha = \frac{y_{water}/y_{ethanol}}{x_{water}/x_{ethanol}}$$

where $y_{water}/y_{ethanol}$ and $x_{water}/x_{ethanol}$ denote the concentration ratio of water and ethanol in the permeate and in the feed, respectively. A constant composition of the feed solution was assumed in each run because the amount of permeate was so small that the change in feed composition was negligible.

Swelling of the Membranes. To evaluate swelling behaviors, PAA-P(BMA50-*co*-MMA50) IPN membranes were prepared as follows.

X-P(BMA50-*co*-MMA50)$_{40}$ (with theoretical $\overline{M_c}$ of 40,000) membranes prepared at 80 °C without solvent. For PAA$_2$-P(BMA50-*co*-MMA50)$_{40}$, the x-P(BMA50-*co*-MMA50)$_{40}$ membrane was immersed in AA mixture containing AA, EGDMA(with theoretical $\overline{M_c}$ of 2,000) and 1 wt% BPO. After 24 hrs, the swollen membranes were placed in convection oven and polymerized at 80 °C for 24 hrs. The same procedure was employed for the preparation of PAA$_{40}$-P(BMA50-*co*-MMA50)$_{40}$ IPN membrane.

The equilibrium-swelling ratios of the x-PBMA, [x-P(BMA-*co*-MMA)] sublayers and PAA-P(BMA-*co*-MMA) IPN membranes were determined by checking weight changes of sublayer samples swollen with water-ethanol mixtures in every 10~30 min, until no incremental weight change was observed. The sample strips were kept for 24 hrs, at room temperature, in glass tubes containing different ethanol aqueous solutions. After the strip was taken out from the liquid and carefully wiped with filter paper to remove the surface liquid, they were weighed as quickly as possible. The swelling ratio (S) of the sample was obtained using the expression $S = (W_s - W_o)/W_o$, where W_o and W_s denote the weights of the dried and swollen samples respectively.

Results and Discussion

Characterization of the Composite Membrane.

SEM Photographs: Figure 3 shows morphologies of composite membrane having PAA-P(BMA-*co*-MMA) IPN skin layer and crosslinked porous P(BMA-*co*-MMA) sublayer. In this membrane, the $\overline{M_c}$ of PAA and PBMA were

40,000, and the sublayer was prepared by polymerizing of mixture having 20 wt% BMA, 20 wt% MMA, 60 wt% NMP and crosslinking agent [i.e. PAA_{40}-P(BMA20-*co*-MMA20)$_{40}$ IPN]. The T_g of polymer was about 70 °C. For this composite membrane (Figure 3), the thickness of the skin layer is not clear and the porosity of the crosslinked sublayer was significantly decreased to an average pore size with 0.2~0.3 μm. The interconnectivity between pores was also decreased compared to x-P(BMA20-*co*-MMA20)$_{40}$ prepared without IPN skin layer (Figure 3(d)). It is thought that the decrease of porosity and interconnectivity were caused by the slowing down of solvent nonsolvent exchange rate due to dense IPN skin layer.

Figure 4 shows the morphologies of the composite membrane x-P(BMA-*co*-MMA) sublayer which was prepared by polymerizing monomer mixture having 15 wt% BMA, 15 wt% MMA, 70 wt% NMP and crosslinking agent. In this case, the $\overline{M_c}$ of PAA was 2,000 and $\overline{M_c}$ of P(BMA-*co*-MMA) was 40,000 [i.e. PAA_2-P(BMA15-*co*-MMA15)$_{40}$ IPN]. Figure 5 shows the morphologies of PAA_2-P(BMA25-*co*-MMA5)$_{40}$ IPN composite membrane. The thicknesses of the skin layers were about 10 μm for PAA_2-P(BMA15-*co*-MMA15)$_{40}$ membrane and about 5~6 μm for PAA_2-P(BMA25-*co*-MMA5)$_{40}$ membrane. We can see sublayer morphologies having well-developed macrovoids and bi-continuous cellular structure.

AFM Images: The surface structures of porous x-P(BMA-*co*-MMA) sublayer and PAA-P(BMA-*co*-MMA) IPN composite membrane imaged by AFM are shown in Figure 6. The view angle is 45 degree, which emphasizes the three dimensional feature of the AFM images. The covering area of Figure 6 is 3 μm × 3 μm. We can see the clear difference between the two membrane surfaces. In the case of sublayer (Figure 6(a)), there exist large pores throughout the whole membrane surface. However, after the sublayer was coated with PAA and IPN structure was formed on the top layer, there was no pore and very smooth surface was observed (Figure 6(b)).

Figure 7 shows the top view and line profile of the membranes. We can see the roughness of the surface decreased considerably after coating the skin layer. From the line profile, we can determine the pore size of sublayer and the result shows that the diameter of three different pores measured are around 145~220 nm.

FT-IR Spectra: The FT-IR spectra of PAA-P(BMA-*co*-MMA) IPN composite membrane are presented in Figure 8. The strong absorption at 1740 cm^{-1} is assigned to the C=O stretching vibration of the ester groups in the PAA and poly

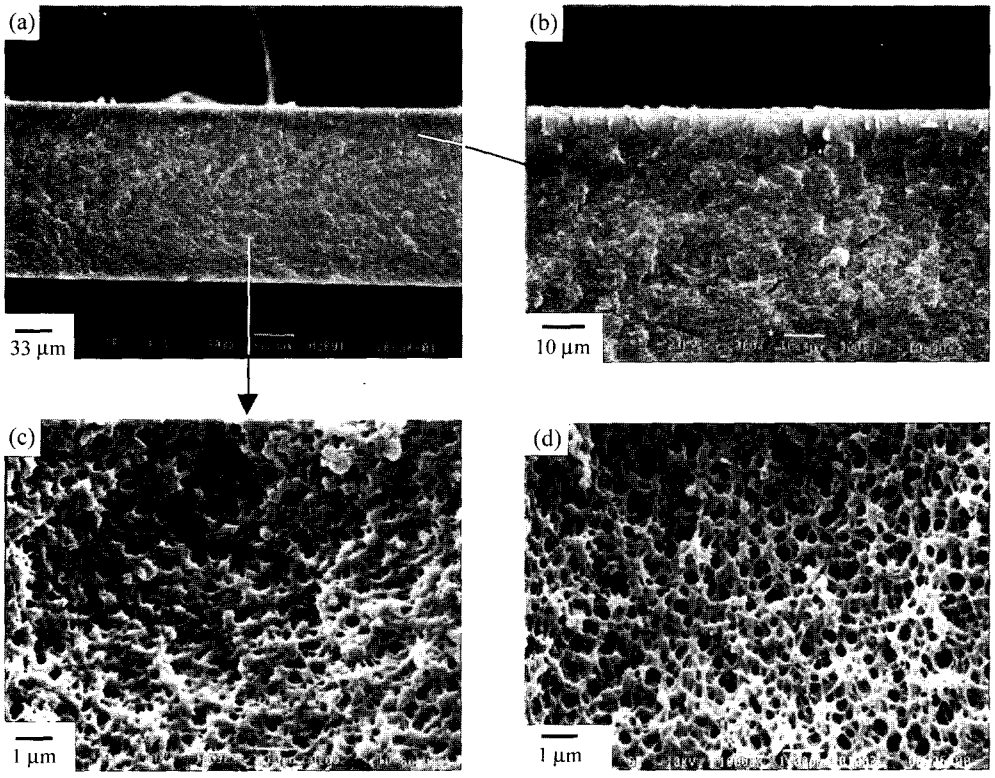

Figure 3. SEM micrographs of the cross-sections for PAA_{40}-P(BMA20-*co*-MMA20)$_{40}$ IPN composite membrane: (a) cross-section of the membrane; (b) PAA_{40}-P(BMA20-*co*-MMA20)$_{40}$ IPN/x-P(BMA20-*co*-MMA20)$_{40}$ interface; (c) cross-section of porous crosslinked P(BMA20-*co*-MMA20)$_{40}$ [$\overline{M_c}$ = 40,000 for PAA and P(BMA-*co*-MMA)]; (d) cross-section of porous crosslinked P(BMA20-*co*-MMA20)$_{40}$ prepared without coating of the skin layer.

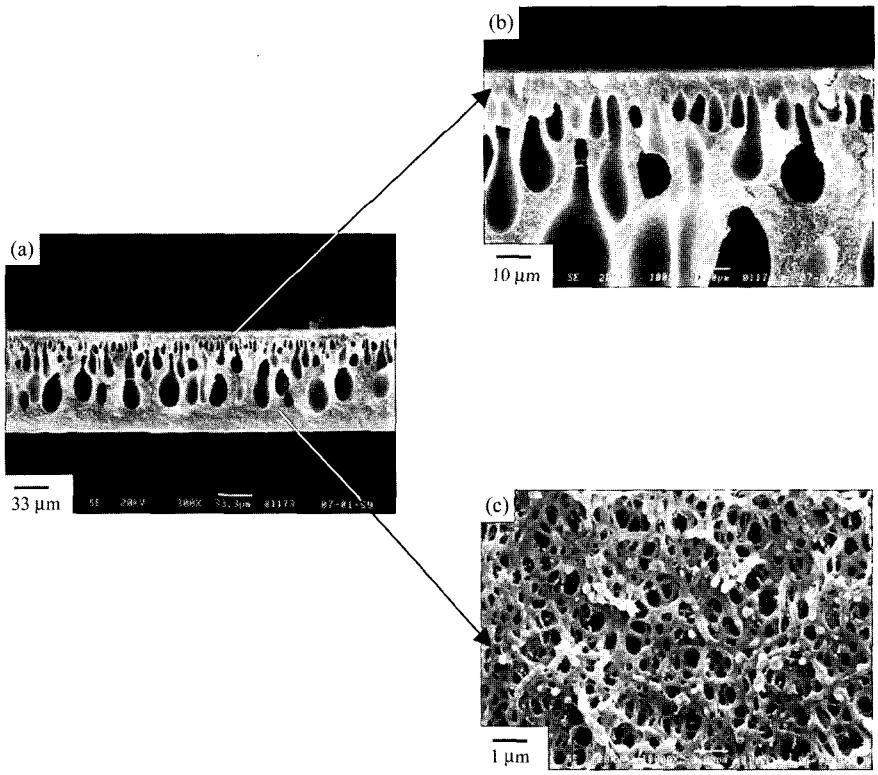

Figure 4. SEM micrographs of the cross-sections for PAA_2-P(BMA15-*co*-MMA15)$_{40}$ IPN composite membrane: (a) cross-section of the membrane; (b) PAA_2-P(BMA15-*co*-MMA15)$_{40}$ IPN/x-P(BMA15-*co*-MMA15)$_{40}$ interface; (c) cross-section of porous crosslinked P(BMA15-*co*-MMA15)$_{40}$ [$\overline{M}_c$ = 2,000 for PAA and $\overline{M}_c$ = 40,000 for P(BMA-*co*-MMA)].

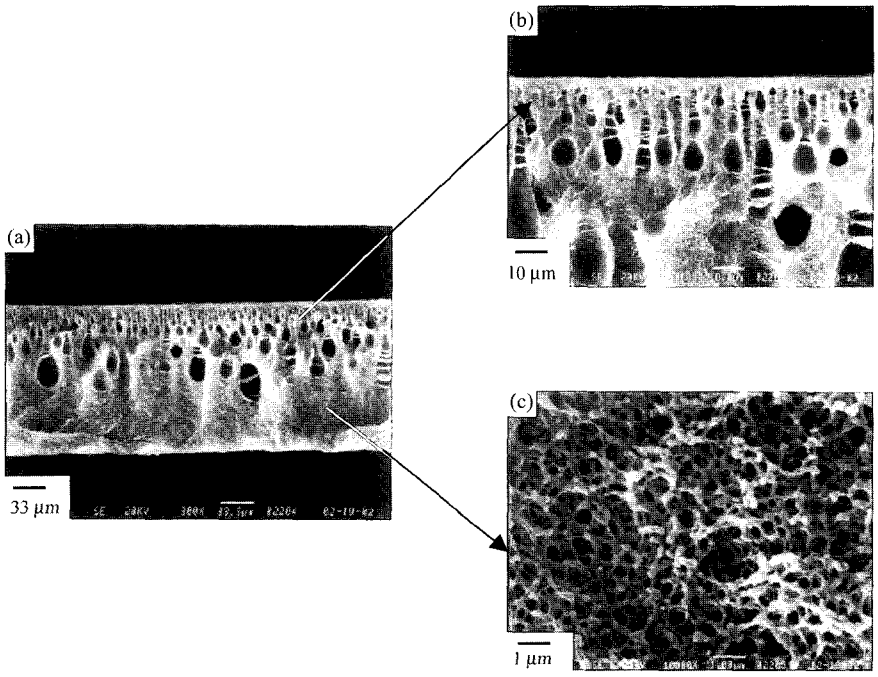

Figure 5. SEM micrographs of the cross-sections for PAA_2-P(BMA25-*co*-MMA5)$_{40}$ IPN composite membrane: (a) cross-section of the membrane; (b) PAA_2-P(BMA25-*co*-MMA5)$_{40}$ IPN/x-P(BMA25-*co*-MMA5)$_{40}$ interface; (c) cross-section of porous crosslinked P(BMA25-*co*-MMA5)$_{40}$ [$\overline{M}_c$ = 2,000 for PAA and $\overline{M}_c$ = 40,000 for P(BMA-*co*-MMA)].

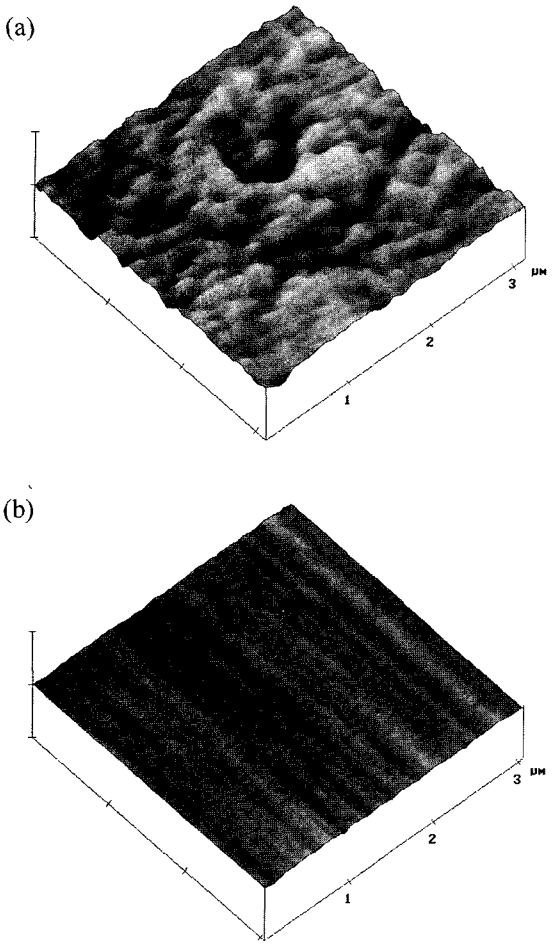

Figure 6. Three dimensional tapping mode AFM images: (a) x-P(BMA15-*co*-MMA15)$_{40}$ sublayer and (b) PAA$_2$-P(BMA15-*co*-MMA15)$_{40}$ IPN composite membrane.

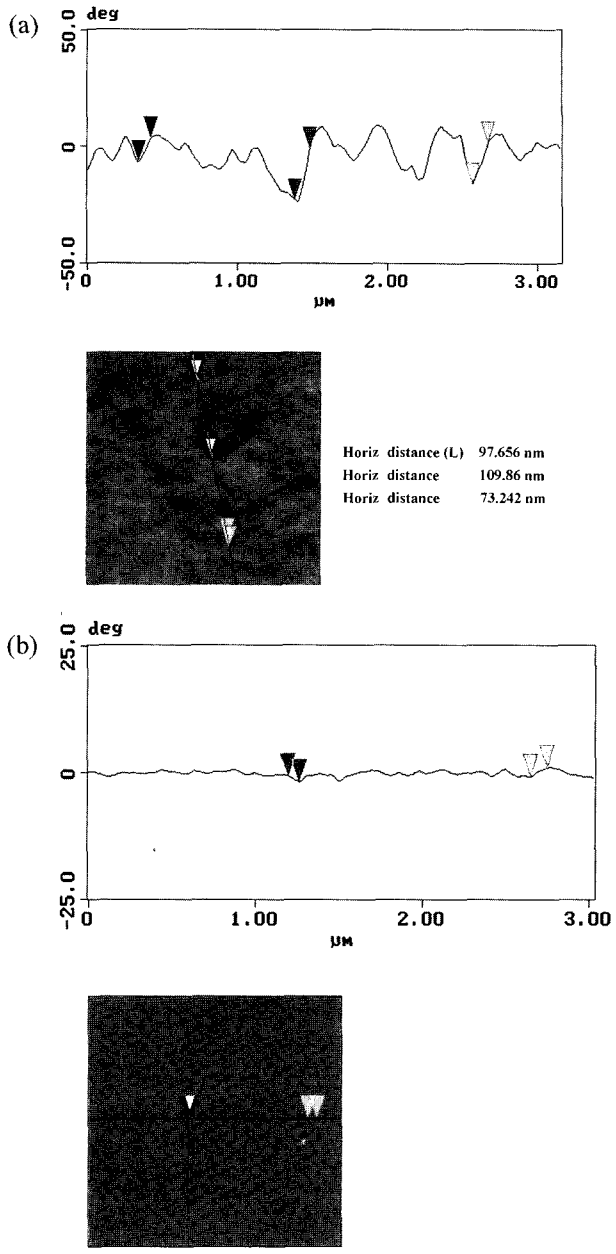

Figure 7. A top view and a line profile of membrane surface taken with AFM: (a) x-P(BMA15-*co*-MMA15)$_{40}$ sublayer and (b) PAA$_2$-P(BMA15-*co*-MMA15)$_{40}$ IPN composite membrane.

(BMA-*co*-MMA) chain. The peak centered at 1565 cm^{-1} represents COO^- (asymmetric stretch) resulting from neutralization. Before neutralization, there is no peak at 1565 cm^{-1}, but after neutralization the peak appears at 1565 cm^{-1}. This shows that on the carboxyl groups of PAA anionic charges were introduced. But the peak at 1565 cm^{-1} is very small compared to that corresponds to the C=O vibration, which means PAA skin layer that can be ionized is relatively thin.

Pervaporation of the Water-Ethanol Mixtures.

Effect of Sublayer Morphology: The permeation rates and separation factors for PAA$_{40}$-P(BMA-*co*-MMA)$_{40}$ IPN composite membranes having different sublayer morphology are shown in Figure 9. It was found that the PAA$_{40}$-P(BMA15-*co*-MMA15)$_{40}$ IPN composite membrane had higher permeation rate than the PAA$_{40}$-P(BMA20-*co*-MMA20)$_{40}$ IPN composite membrane throughout the whole feed composition but the difference of the separation factors between the two membranes were not so significant. From this observation, we can see that the permeation rates are closely related with sublayer thickness and sublayer morphology (Figures 3, 4), but separation factor is not influenced largely by the sublayer structure. Figures 3 and 4 indicate the clear difference of sublayer morphologies between the two membranes. PAA$_2$-P(BMA15-*co*-MMA15)$_{40}$ IPN composite membrane had high porosity and bi-continuous interconnected pore structure. For different $\overline{M}_c$(40,000) of PAA with the same sublayer composition (i.e. PAA$_{40}$-P(BMA15-*co*-MMA15)$_{40}$ IPN), the crosslinked and porous sublayers

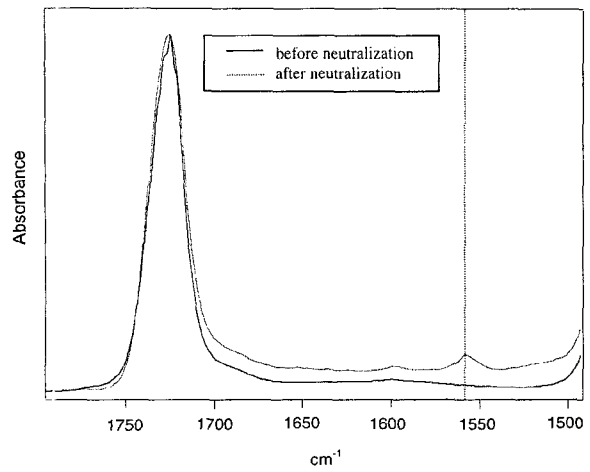

Figure 8. FT-IR spectra of PAA-P(BMA-*co*-MMA) IPN membrane before and after neutralization.

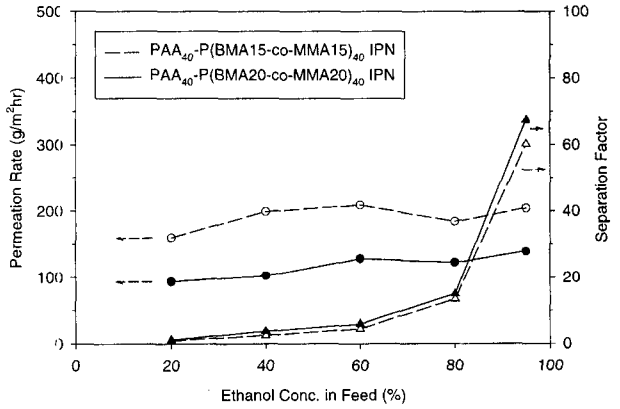

Figure 9. Pervaporation performance of IPN composite membranes having different sublayer morphologies at 25 °C.

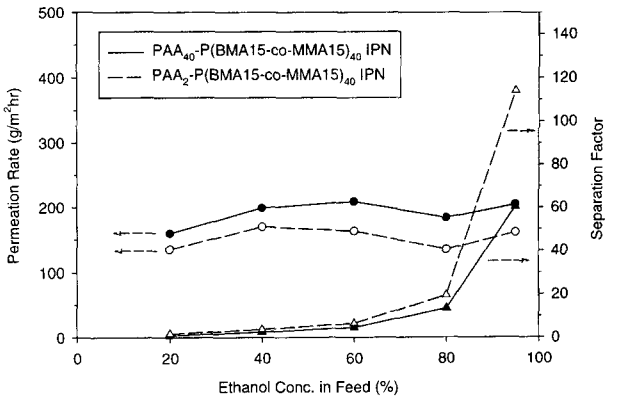

Figure 10. Effects of degree of crosslinking on pervaporation performance for PAA-P(BMA15-*co*-MMA15)$_{40}$ IPN composite membranes at 25 °C.

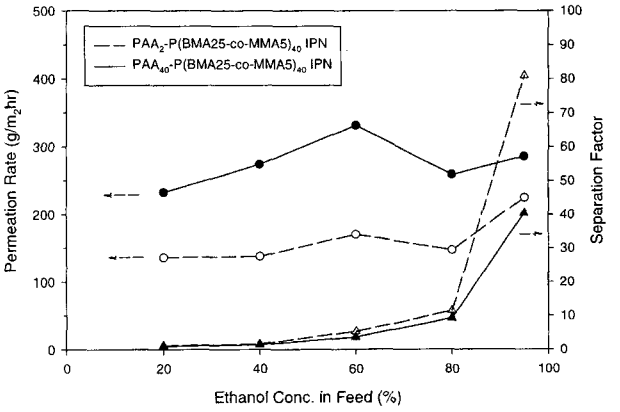

Figure 11. Effects of degree of crosslinking on pervaporation performance for PAA-P(BMA25-*co*-MMA5)$_{40}$ IPN composite membranes at 25 °C.

exhibited little change in its morphologies compared to that of PAA$_2$-P(BMA15-*co*-MMA15)$_{40}$ IPN composite membrane. The porosities of the PAA$_{40}$-P(BMA20-*co*-MMA20)$_{40}$ and PAA$_{40}$-P(BMA15-*co*-MMA15)$_{40}$ IPN composite membranes were 40.1% and 58.0% respectively.

Effect of Crosslinking Density: Figures 10 and 11 show the effect of crosslink density of two IPN membranes having different skin layer. At the same ethanol concentration in the feed, the permeation rates increase with the increase of the $\overline{M_c}$ of x-PAA. However, the separation factors decrease with the increase of the $\overline{M_c}$ of x-PAA. This is due to the increased swelling of the skin layer with the increase of $\overline{M_c}$ of x-PAA. The increased mobility of water and ethanol results in the decrease of selectivity of the water. This phenomenon is very general in the pervaporation performance for water-ethanol separation.[13,15,16] In the case of PAA$_2$-P(BMA15-*co*-MMA15)$_{40}$ IPN composite membrane, the separation factor was 114 and permeation rate was 160 g/m^{2}hr at 95% ethanol feed. The separation factor of the PAA$_2$-P(BMA15-*co*-MMA15)$_{40}$ membrane increased about twice as that of PAA$_{40}$-P(BMA15-*co*-MMA15)$_{40}$ IPN composite membrane, but the permeation rate decreased about 20%. PAA$_2$-P(BMA25-*co*-MMA5)$_{40}$ IPN membrane shows relatively high permeation rates than PAA$_2$-P(BMA15-*co*-MMA15)$_{40}$ IPN membrane. It is thought that this comes from the relatively thin skin layer in PAA$_2$-P(BMA25-*co*-MMA5)$_{40}$ membrane (Figure 5).

Effect of Anionic Charges of Skin Layer: Several studies show that water selectivity is enhanced by introducing ionized groups into the membrane.[5,17,18] This can be accounted for the fact that ionized groups hydrate strongly and exclude organic solvents. Figure 12 presents pervaporation characteristics in PAA$_2$-P(BMA25-*co*-MMA5)$_{40}$ IPN and anionic PAA$_2$-P(BMA25-*co*-MMA5)$_{40}$ IPN composite membranes. The permeation rate of anionic IPN membrane is much higher than nonionic IPN membrane throughout the whole

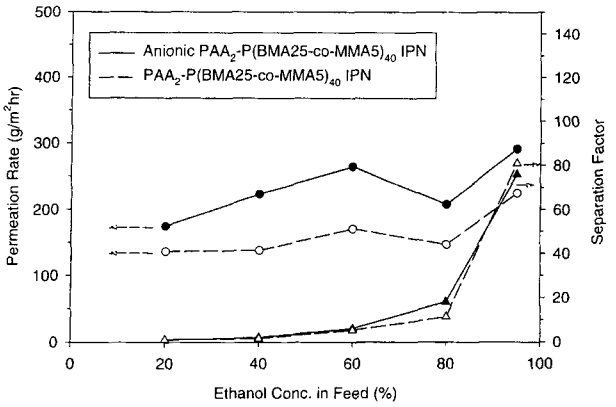

Figure 12. Effects of anionic charges on pervaporation performance for PAA_2-P(BMA25-*co*-MMA5)$_{40}$ IPN composite membranes at 25 °C.

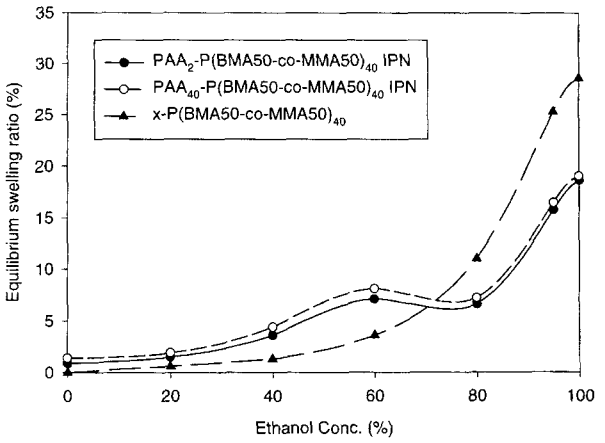

Figure 13. Equilibrium swelling behavior of PAA-P(BMA-*co*-MMA) IPN and x-P(BMA-*co*-MMA) sublayer in water-ethanol mixtures at 25 °C.

ethanol concentration, but the separation factors are similar. This can be explained by the observation that the membrane containing sodium carbixylates had higher pervaporation performance than the membrane with carboxylic acids groups.[15] Strong affinity with water due to anionic charge possibly enhances selectivity, but in this system it is thought that the mutual association between permeant molecules especially at low temperature resulted in flux increase rather than selectivity enhancement.

Effect of the Feed Composition: The pervaporation characteristics of the PAA-P(BMA-*co*-MMA) IPN composite membranes show quite similar behavior each other (Figures 9-12). The selectivity increases with ethanol content in the feed mixture, but permeation rate varies depending on the composition. The permeation rate shows a maximum at 60 wt% ethanol concentration and shows a minimum at 80 wt% ethanol concentration for all the PAA-P(BMA-*co*-MMA) IPN composite membranes.

To compare the permeation behavior with the swelling behavior of the IPN skin layer, several PAA-P(BMA-*co*-MMA) IPN membranes prepared by polymerization without solvent. The amounts of PAA were about 8 wt% for both PAA_2-P(BMA50-*co*-MMA50)$_{40}$ and PAA_{40}-P(BMA50-*co*-MMA50)$_{40}$ membranes. Swelling behaviors of PAA-P(BMA50-*co*-MMA50)$_{40}$ IPN membranes as a function of ethanol concentration in water ethanol mixtures give some indication about the permeability behavior of the composite membrane (Figure 13). In Figure 13, the swelling ratio of the crosslinked P(BMA50-*co*-MMA50)$_{40}$ sublayer was also included. The swelling ratio of x- P(BMA50-*co*-MMA50)$_{40}$ increases monotonously with the ethanol concentration, but PAA-P(BMA50-*co*-MMA50) IPN membranes show a maximum at 60 wt% ethanol and a minimum at 80 wt% ethanol concentration. The swelling ratios of the two IPN membranes having different degree of crosslinking show slight difference, which is quite different with the result of pervaporation behavior (Figures 10, 11). This can be accounted by the fact that the PAA concentration in these IPN membranes were small as 8 wt% and there exists a difference of swelling characteristics between the solution-crosslinked polymer and bulk-crosslinked polymer.

Conclusions

The PAA-P(BMA-*co*-MMA) composite membranes having IPN skin layer supported on porous and crosslinked sublayer were prepared. The morphology of the sublayer of the composite membrane prepared in the presence of 60 wt% solvent showed cellular structure, on the other hand that of sublayer prepared in the presence of 70 wt% solvent presented interconnected pore structure with macrovoids. The skin layer thickness of the PAA-P(BMA-*co*-MMA) IPN composite membrane was about 10 μm, and using AFM images it was found that the skin layer has no defect.

For the azeotropic water-ethanol mixture (95 wt% ethanol), the PAA_2-P(BMA15-*co*-MMA15)$_{40}$ IPN composite membranes had separation factor of 114 and permeation rate of 160 g/m^{2}hr at 25 °C. Permeation rates were largely influenced by the morphology of the sublayer. Separation factors increased and permeation rates decreased with the increase of degree of crosslinking of the PAA. It was found that permeation rates could be increased by introducing anionic charges on carboxyl groups of the PAA. Permeation rate was maintained even at high ethanol concentration. The permeation rate behavior of the PAA-P(BMA-*co*-MMA) IPN composite membranes showed similar behavior with the swelling ratio of the IPN skin layer.

Acknowledgements. This study was supported by the Center for Advanced Functional Polymers, which was funded by the Korean Science & Engineering Foundation (KOSEF), Daejeon, Korea.

References

(1) Y. D. Kim, B. K. Lee, E. J. Jeon, Y. C. Shin, and S. C. Kim, *Macromol. Symp.*, **98**, 665 (1995).
(2) T. Q. Nguyen, A. Essamri, R. Clement, and J. Neel, *Macromol. Chem.*, **188**, 1973 (1987).
(3) L. H. Spering, Interpenetrating Polymer Networks and Related Materials, Plenum Press, New York and London , 1981.
(4) J. H. Lee and S. C. Kim, *Macromol.*, **19**, 644 (1986).
(5) C. E. Reineke, J. A. Jagodzinski, and K. R. Denslow, *J. Membr. Sci.*, **32**, 207 (1987).
(6) A. Wenzlaff, K. W. Böddeker, and K. Hattenbach, *J. Membr. Sci.*, **22**, 333 (1985).
(7) Y. K. Lee, T. M. Tak, D. S. Lee, and S. C. Kim, *J. Membr. Sci.*, **52**, 157 (1990).
(8) M. J. Lee, B. H. Lim, and W.Y. Kim, *Polymer (Korea)*, **19**, 317 (1995)
(9) E. J. Jeon and S. C. Kim, *J. Membr. Sci.*, **70**, 193 (1992).
(10) L. Liang and E. Ruckenstein, *J. Membr. Sci.*, **114**, 227 (1996).
(11) H. Karakane, M. Tsuyumoto, Y. Maeda, and Z. Honda, *J. Appl. Poly. Sci.*, **42**, 3229 (1991).
(12) H. S. Choi, T. Hino, M. Shibata, Y. Negishi, and H. Ohya, *J. Membr. Sci.*, **72**, 259 (1992).
(13) M. Yoshikawa, T. Yukoshi, K. Sanui, and N. Ogata, *J. Polym. Sci.*: Part A: Polym. Chem., **24**, 585 (1986).
(14) B. Y. Lim and S. C. Kim, *J. Membr. Sci.*, **209**, 293 (2002).
(15) Y. S. Kang, S. W. Lee, U. Y. Kim, and J. S. Shim, *J. Membr. Sci.*, **51**, 215 (1990).
(16) E. Ruckenstein and L. Liang, *J. Membr. Sci.*, **110**, 99 (1996).
(17) I. Cabbasso and Z. Liu, *J. Membr. Sci.*, **24**, 101 (1985).
(18) A. Wenzlaff, K. W. Böddeker, and K. Hattenbach, *J. Membr. Sci.*, **22**, 333 (1985).